

## Review Article

# A Fully Coupled Hydromechanical Model for CO<sub>2</sub> Sequestration in Coal Seam: the Roles of Multiphase Flow and Gas Dynamic Diffusion on Fluid Transfer and Coal Behavior

Rui Yang,<sup>1,2</sup> Weiqun Liu ,<sup>1,2</sup> Tianran Ma,<sup>1,2</sup> Junhe Xie,<sup>2</sup> Yang Hu,<sup>1,2</sup> Rui Zhou,<sup>3,4</sup> and Yongjie Yang <sup>5</sup>

<sup>1</sup>State Key Laboratory Geomechanics and Deep Underground Engineering, China University of Mining and Technology, Xuzhou, Jiangsu 221116, China

<sup>2</sup>School of Mechanics and Civil Engineering, China University Mining and Technology, Xuzhou, Jiangsu 221116, China

<sup>3</sup>State Key Laboratory of Coal Mine Safety Technology, CCTEG Shenyang Research Institute, Fushun 113000, China

<sup>4</sup>Key Laboratory of Ministry of Education on Safe Mining of Deep Metal Mines, Northeastern University, Shenyang 110000, China

<sup>5</sup>College of Energy and Mining Engineering, Shandong University of Science and Technology, Qingdao, Shandong 266590, China

Correspondence should be addressed to Weiqun Liu; [weiqun\\_liu@126.com](mailto:weiqun_liu@126.com)

Received 9 August 2020; Revised 25 August 2020; Accepted 9 September 2020; Published 24 September 2020

Academic Editor: Zhijie Wen

Copyright © 2020 Rui Yang et al. This is an open access article distributed under the Creative Commons Attribution License, which permits unrestricted use, distribution, and reproduction in any medium, provided the original work is properly cited.

CO<sub>2</sub> sequestration in coal seam has proved to be an effective way for reducing air pollution caused by greenhouse gases. A study on the rules of fluid transfer and reliability of CO<sub>2</sub> storage during gas injection is necessary for the engineering application. However, the clarification of multifield coupling in long-term CO<sub>2</sub> sequestration is the difficulty to solve the aforementioned problem. Previous investigations on the coupled model for CO<sub>2</sub> storage in coal seam were not exactly comprehensive; for example, the multiphase flow in the fracture and the nonlinear behavior of gas diffusion were generally neglected. In this paper, a new multistage pore model of the coal matrix and the corresponding dynamic diffusion model were adopted. Meanwhile, the CO<sub>2</sub>-induced coal softening and the CO<sub>2</sub>-water two-phase flow in coal fracture were also taken into account. Subsequently, all the mentioned mechanisms and interactions were embedded into the coupled hydromechanical model, and this new fully coupled model was well verified by a set of experimental data. Additionally, through the model application for long-term CO<sub>2</sub> sequestration, we found that the stored CO<sub>2</sub> molecules are mainly in an adsorbed state at the early injection stage, while with the continuous injection of gas, the stored CO<sub>2</sub> molecules are mainly in a free state. Finally, the roles of multiphase flow and gas dynamic diffusion on fluid transfer and coal behavior were analyzed. The results showed that the impact of multiphase flow is principally embodied in the area adjacent to the injection well and the coal seam with lower initial water saturation is more reliable for CO<sub>2</sub> sequestration, while the impact of gas dynamic diffusion is principally embodied in the area far away from the injection well, and it is safer for CO<sub>2</sub> sequestration in coal seam with greater attenuation coefficient of CO<sub>2</sub> diffusion.

## 1. Introduction

With the rapid development of human society industrialization, the anthropogenic emissions of greenhouse gases (GHG) such as CO<sub>2</sub> are escalating, which is believed as a primary cause for global climate change [1]. In this respect, the United Nations Intergovernmental Panel on Climate Change

(IPCC) recommends utilizing Carbon Capture and Storage (CCS) technology to cut GHG emissions drastically [2]. At present, several potential methods for CO<sub>2</sub> storage have been proposed, including geological sequestration [3], oceanic sequestration [4], and mineralized sequestration [5]. Among these options, CO<sub>2</sub> sequestration in unminable coal seams is the most concerned one worldwide because of its multiple

benefits [6]. Therefore, an applicable model for predicting storage efficiency and analyzing coal behavior during CO<sub>2</sub> injection is urgently needed.

The process of CO<sub>2</sub> sequestration in coal seam can be described as follows: firstly, the CO<sub>2</sub> discharged from industry is cooled and compressed into liquid or supercritical state; then, the processed CO<sub>2</sub> is transported and injected into deep coal seam through a pipeline; and finally, the injected CO<sub>2</sub> is stored in the coal seam under adsorbed state or free state after multiple mechanisms of migration, such as Darcy's flow, diffusion, and adsorption [7]. In addition, based on a previous study, the coal mechanical properties have a significant impact on CO<sub>2</sub> transfer and storage in coal seam [8], and the injected CO<sub>2</sub> also has a strong feedback on coal mechanical behavior [9]. This complex coupled process can cause difficulties in modeling long-term CO<sub>2</sub> sequestration in the coal seam. To date, there are various models that have been proposed under different assumptions. Wu et al. [10] established a coupled hydromechanical model to investigate the change of coal permeability induced by CO<sub>2</sub> injection. They viewed the coal seam as a dual-porosity dual-permeability media and found that the interactions between the fracture system and matrix system are crucial for analyzing the CO<sub>2</sub> migration in coal seam. Qu et al. [11] embedded the temperature effect into the model of Wu et al. [10] and further revealed the impact of internal fractures on coal permeability during CO<sub>2</sub> sequestration. Additionally, several models for CO<sub>2</sub> geological sequestration with different coupling relations have also been proposed in recent years. Masoudian et al. [12] developed a fully coupled model of coal deformation and gas flow. Based on a parametric study, the researchers believed that the elastic modulus is the most primary coal property in clarifying the process of CO<sub>2</sub> storage. Fan et al. [13] considered the thermal field in the existing gas-solid coupling model and found that the coal swelling or shrinkage induced by temperature change could not be neglected in modeling coal permeability and CO<sub>2</sub> storage efficiency. Further, Zhang et al. [14] derived a coupled thermal-hydrological-mechanical-chemical model by taking gas dissolution and chemical reactions into account. They showed that the model contenting more related factors has more accuracy in predicting CO<sub>2</sub> injection rate and studying the mechanical behavior of coal.

Although considerable models have been proposed, there are still two imperfections in the recent studies. The first is that the effect of groundwater is usually neglected. Based on Fan et al.'s [15] study, the initial water saturation in coal seam plays a significant role in CO<sub>2</sub> sequestration or CO<sub>2</sub> enhanced coalbed methane recovery. The preexisting water can complicate the fluid flow during CO<sub>2</sub> sequestration in coal as a result of the interaction between the gas phase and liquid phase, which is mainly reflected by relative permeability [16]. Additionally, many theoretical and experimental studies have found that the relative permeability of gas or water is controlled by water saturation, as shown in Figure 1. The results illustrate that although the values of relative permeability obtained by different investigations are not identical, they have the same variation trend with water saturation. It is obvious the migration ability of gas in coal

seam with higher water saturation is extremely low, thus disregarding the original water of the reservoir may overvalue the CO<sub>2</sub> storage rate grossly.

The second imperfection is that the prior models did not address the complex dynamic diffusion of CO<sub>2</sub> in coal. But in fact, the nonlinear diffusion process of gas in coal matrix pore has been widely reported in previous investigations [24–26]. Liu et al. [27] introduced a dynamic diffusion model which the diffusion coefficient attenuates with time, and the model has been verified by experimental results and field test data of coalbed methane recovery. In addition, Clarkson and Bustin [28] conducted a series of experiments for determining CO<sub>2</sub> diffusivities in coal under different pore structure and gas pressure. The results indicated that the CO<sub>2</sub> diffusion in the coal matrix may not be a steady-state process and is largely dependent upon the pore structure and distribution. Therefore, to analyze the fluid flow in coal seam during CO<sub>2</sub> geological sequestration and reveal the mechanical characteristic alterations induced by CO<sub>2</sub> injection, an applicable coupled model, which considers multiphase flow and dynamic diffusion of gas, must be developed first.

This paper establishes a fully coupled CO<sub>2</sub>-water-coal multiphase model in which the CO<sub>2</sub> diffusion coefficient is dependent on the pore size of the coal and diffusion time. Young's modulus and Poisson's ratio of coal are also varied with the amount of the adsorbed CO<sub>2</sub> in coal according to a set of experimental results. In addition, the impacts of multiphase flow and gas dynamic diffusion on CO<sub>2</sub> storage efficiency and coal behavior were analyzed accordingly. Our investigation can improve the understanding of gas-water-coal interactions under complex coupling and better evaluate the reliability of storage conditions after CO<sub>2</sub> injection.

## 2. A Fully Coupled Hydromechanical Model with CO<sub>2</sub>-Water Two-Phase Flow

Aiming at comprehensively clarifying the complex coupled process during CO<sub>2</sub> geological sequestration, in this section, four governing equations and a set of coupling relations are developed, including coal deformation, gas diffusion in coal matrix, two-phase flow in coal fracture, CO<sub>2</sub>-induced softening in coal, adsorption-induced coal swelling and stress-induced permeability alternations in coal fracture.

*2.1. CO<sub>2</sub> Diffusion in Coal Matrix.* The diffusion and adsorption of gas in coal is the main reason why coal seam can capture and store CO<sub>2</sub>. Thus, describing the diffusion behavior of CO<sub>2</sub> in the coal matrix accurately is vitally important in making exactly the prediction of CO<sub>2</sub> geosequestration. Typically, the unipore diffusion model is adopted to express the gas diffusion in porous media, as shown in Figure 2(a). For this model, the diffusion coefficient is constant at any time of CO<sub>2</sub> storage (see in Figure 2(b)). But in fact, the pore structure and distribution of coal are complex and the fractal characteristics of the pore have been widely reported in recent years [29–31]. Based on these investigations, a new diffusion model with a multistage diffusion path was developed by Li et al. [32], which is illustrated in Figure 2(c). For the new proposed model, the pore structure has obvious

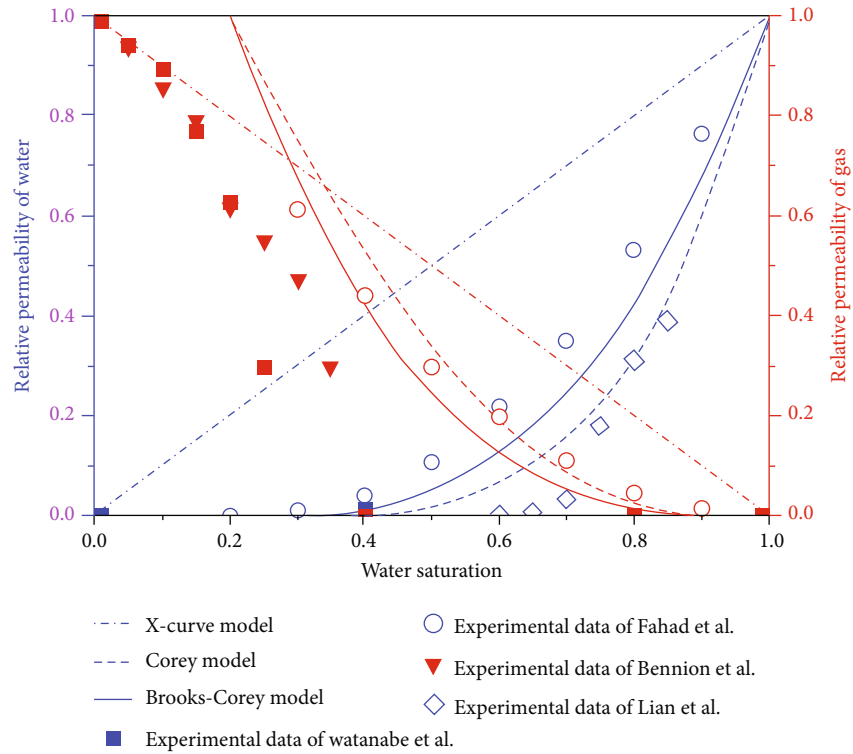


FIGURE 1: Results of relative permeability from Watanabe et al. [17], Fahad et al. [18], Bennion and Bachu [19], and Lian et al. [20]. Several traditional relative permeability models, such as the X-curve model [21], Corey model [22], and Brooks-Corey model [23] are also shown. (Note: For the same symbol, red refers to gas relative permeability, while blue refers to water relative permeability.)

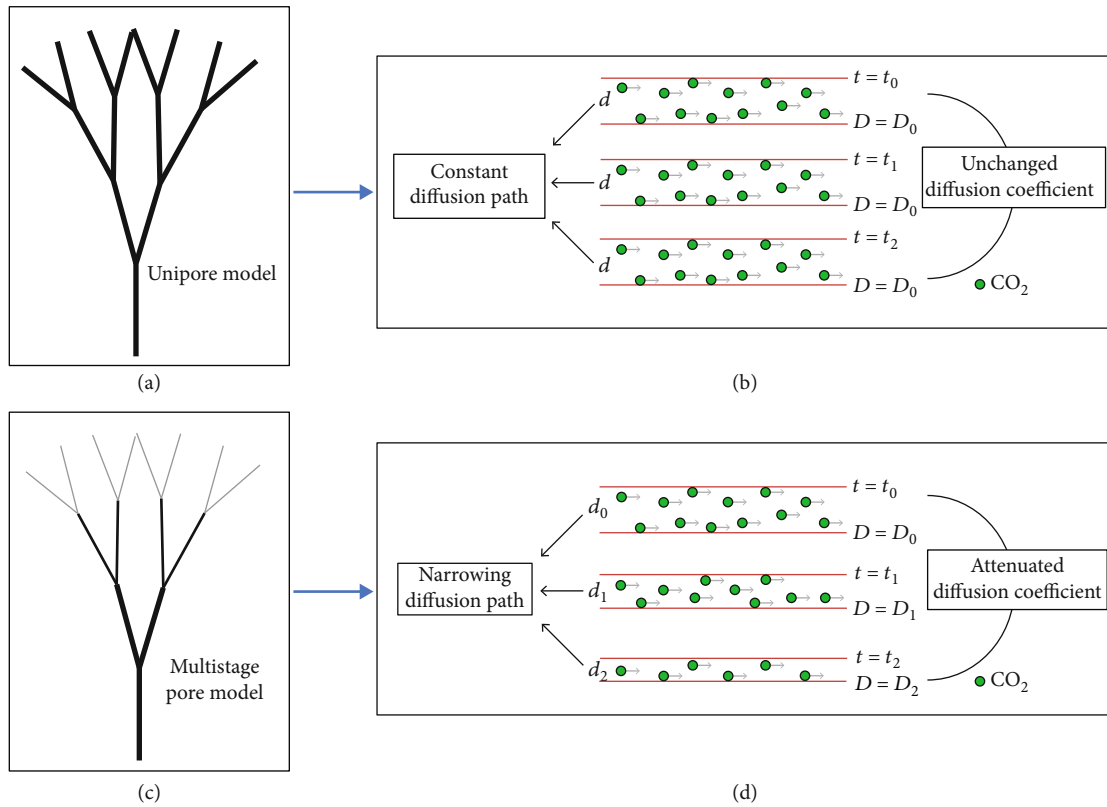


FIGURE 2: Two different models for CO<sub>2</sub> diffusion in coal matrix pore.

fractal properties on a specific scale, and the CO<sub>2</sub> diffusion coefficient varies with time because of the narrowing diffusion path (see in Figure 2(d)). Additionally, according to the experimental results from Liu and Lin [33], the gas dynamic diffusion coefficient considering the fractal properties of the pore can be expressed as the following equation:

$$D_t = D_0 \exp(-\beta t), \quad (1)$$

where  $D_0$  is the initial diffusion coefficient of CO<sub>2</sub>, and  $\beta$  represents the attenuation coefficient. Therefore, the existing governing equation for CO<sub>2</sub> diffusion [34, 35] evolves as follows:

$$\varphi_m \frac{M}{RT} \frac{\partial p_m}{\partial t} + \frac{\rho_c \rho_{ga} v_L p_L}{(p_m + p_L)^2} \frac{\partial p_m}{\partial t} = \frac{3\pi^2 M D_0 \exp(-\beta t) (p_{fg} - p_m)}{RTL^2}, \quad (2)$$

here,  $\varphi_m$  is the porosity of the coal matrix,  $p_m$  represents the CO<sub>2</sub> pressure in the matrix,  $p_{fg}$  represents the CO<sub>2</sub> pressure in fracture,  $M$  is the molar mass of CO<sub>2</sub>,  $R$  is the gas molar constant,  $T$  is the temperature,  $\rho_c$  is the density of coal,  $\rho_{ga}$  is the density of CO<sub>2</sub> under standard condition,  $L$  is the average distance between fractures of coal, and  $v_L$  and  $p_L$  represent the Langmuir volume constant and Langmuir pressure constant, respectively. In Eq. (2), the first term of the left side represents the mass change of free gas, the second term of the left side represents the mass change of the adsorbed gas, and the right side represents the CO<sub>2</sub> diffusion between the coal matrix and fracture, which is defined as a nonlinear process in this paper.

**2.2. Two-Phase Flow in Fracture.** As a result of initial water saturation, the fluid flow in coal fracture should be regarded as a two-phase flow process during CO<sub>2</sub> injection. Based on a previous study [36], the mass balance equation for multi-phase flow can be written as:

$$\frac{\partial m_i}{\partial t} + \nabla \cdot (\rho_i \mathbf{u}_i) = Q_i, \quad (3)$$

where  $\mathbf{u}_i$  is the velocity ( $i = g$  or  $w$  represents CO<sub>2</sub> or water, respectively),  $Q_i$  is the flow sinks, and  $m_i$  is the mass of different phases, which can be given as:

$$m_i = \varphi_f s_i \rho_i, \quad (4)$$

here,  $\varphi_f$  is the porosity of fracture, and  $s_i$  represents the gas or water saturation ( $s_w + s_g = 1$ ). In addition, the velocity of fluids can be described by Darcy's law, which is:

$$\mathbf{u}_i = -\frac{k k_{ri}}{\mu_i} \nabla p_{fi}, \quad (5)$$

where  $k$  is the absolute permeability,  $k_{ri}$  is the relative permeability of gas or water, and  $p_{fi}$  represents the gas or water pressure in fracture ( $p_{fg} - p_{fw} = p_c$ ).

In this paper, we assume that the water only exists in the fracture system, while the CO<sub>2</sub> exists in both the fracture system and the matrix system, and the CO<sub>2</sub> in the fracture can further diffuse into the coal matrix. Therefore, the flow sinks for gas and water in the fracture can be expressed as:

$$Q_g = \frac{3\pi^2 M D_0 \exp(-\beta t) (p_m - p_{fg})}{RTL^2}, \quad (6)$$

$$Q_w = 0. \quad (7)$$

Substituting Eqs. (4)–(7) into Eq. (3), we yield the governing equations for CO<sub>2</sub>-water two-phase flow in fracture:

$$\begin{aligned} \frac{\partial \varphi_f s_g \rho_g}{\partial t} - \nabla \cdot \left( \frac{\rho_g k k_{rg}}{\mu_g} \nabla p_{fg} \right) &= \frac{3\pi^2 M D_0 \exp(-\beta t) (p_m - p_{fg})}{RTL^2}, \\ \frac{\partial \varphi_f s_w \rho_w}{\partial t} - \nabla \cdot \left( \frac{\rho_w k k_{rw}}{\mu_w} \nabla p_{fw} \right) &= 0. \end{aligned} \quad (8)$$

**2.3. Relative Permeability.** As mentioned in the Introduction section, the relative permeability is the key factor for controlling the two-phase flow behavior. Several relative permeability curves have been proposed over the last two decades. In this study, the following equations are adopted to describe the relationship between relative permeability and water saturation [26]:

$$S^* = \frac{s_w - s_{wr}}{1 - s_{wr} - s_{gr}}, \quad (9)$$

$$k_{rg} = (1 - S^*)^2 (1 - S^{*2}), \quad (10)$$

$$k_{rw} = \sqrt{S^*} \left[ 1 - (1 - S^{*1/a})^a \right]^2, \quad (11)$$

here,  $S^*$  is the effective saturation,  $s_{wr}$  and  $s_{gr}$  are irreducible saturations of water and gas, respectively, and  $a$  is a coefficient. Further, Figure 3 illustrates the corresponding relative permeability curves.

**2.4. CO<sub>2</sub>-Induced Coal Softening.** The alternations of mechanical properties in coal induced by CO<sub>2</sub> injection are another process which is usually neglected in modeling long-term CO<sub>2</sub> sequestration in the coal seam. And considerable reports have shown that the coal properties, such as Young's modulus and Poisson's ratio, are not negligible for analyzing fluid migration and evaluating the reliability of CO<sub>2</sub> storage. Therefore, embedding the CO<sub>2</sub>-induced coal softening into the coupled model is much-needed.

Aiming to clarify the impact of CO<sub>2</sub> pressure on coal mechanical behavior, Ma et al. [37] conducted a triaxial compression test using coal samples with CO<sub>2</sub> contents. The laboratory data indicates that the sample with high CO<sub>2</sub> pressure exhibits lower Young's modulus and higher Poisson's ratio, as shown in Figure 4. To quantify the change of Young's modulus induced by CO<sub>2</sub> overpressure, we

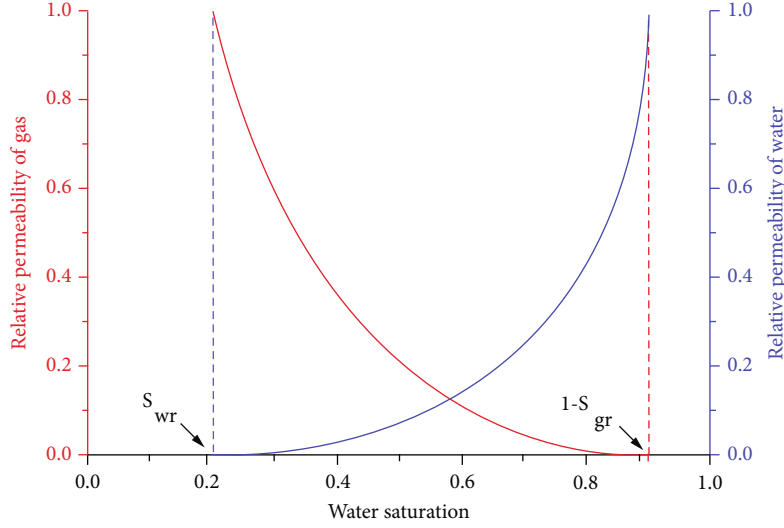


FIGURE 3: Relative permeability curves for two-phase flow.

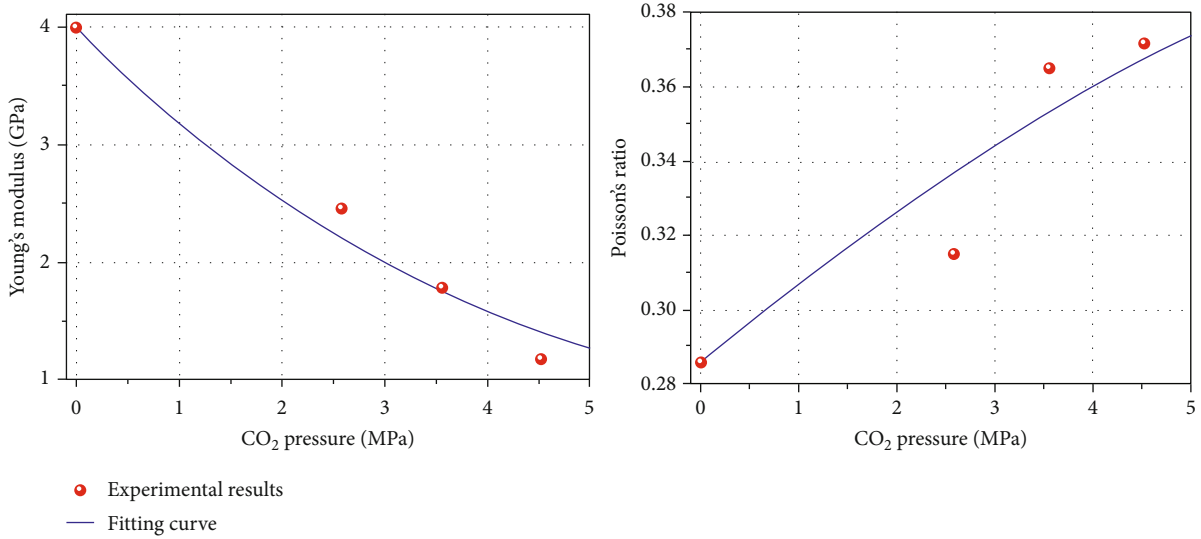


FIGURE 4: Experimental data of Young's modulus and Poisson's ratio at different CO<sub>2</sub> pressures.

propose an exponential equation to fit the experimental results (see in Figure 4), which is written as:

$$E_p = E \exp(-\delta_1 \cdot \Delta p_m), \quad (12)$$

where  $E$  is the initial Young's modulus of coal before CO<sub>2</sub> injection,  $E_p$  is Young's modulus varying with pore pressure of gas, and  $\delta_1$  represents a fitting coefficient related to coal condition, which is equal to 0.2291 in this study according to the experimental data.

Similarly, another exponential equation is introduced to quantify the alternation of Poisson's ratio (see in Figure 4), which is written as:

$$\nu_p = \nu_l + (\nu - \nu_l) \exp(-\delta_2 \cdot \Delta p_m), \quad (13)$$

where  $\nu$  is Poisson's ratio of coal when the overpressure is

zero,  $\nu_p$  is Poisson's ratio varying with pore pressure of gas,  $\nu_l$  is the maximum value of Poisson's ratio, which is set to 0.5 in this study, and  $\delta_2$  represents the fitting coefficient, which is equal to 0.1054.

**2.5. Coal Deformation.** Based on our previous study [26], the governing equation of coal deformation considering two-phase flow, adsorption-induced swelling, and CO<sub>2</sub>-induced softening can be described as:

$$Gu_{i,jj} + \frac{G}{1 - 2\nu_p} - \alpha_m p_{m,i} - \alpha_f p_{f,i} - K\varepsilon_{s,i} + f_i = 0, \quad (14)$$

( $1 - 2\nu_p$ ) is the bulk modulus;  $p_f = s_g p_{fg} + s_w p_{fw}$  is the total fluid pressure in the fracture system;  $\alpha_m$  and  $\alpha_f$  are the Biot coefficients of coal matrix and fracture, respectively; and  $\varepsilon_s$

is the coal strain induced by the CO<sub>2</sub> adsorption, which is defined as:

$$\varepsilon_s = \frac{\varepsilon_L p_m}{p_m + p_L}, \quad (15)$$

here,  $\varepsilon_L$  represents the Langmuir strain constant. Additionally, note that in Eq. (14), Young's modulus and Poisson's ratio are not constant like other references assumed, but vary with CO<sub>2</sub> pressure in the coal matrix.

**2.6. Cross-Coupling.** The interactions between fluid transport and coal deformation are the primary reason why it is difficult to model long-term CO<sub>2</sub> geological sequestration. Fluid transfer in coal seam during CO<sub>2</sub> injection involves multiple mechanisms, such as two-phase flow, gas diffusion, and gas adsorption. All of these processes can cause alternations of stress and strain in the coal seam. In this paper, the change of porosity is adopted to reflect the main impact of the fluid transfer on the mechanical properties of coal. And mutually, the change of porosity also has a strong feedback on coal permeability. According to cubic law and the investigation of Ma et al. [36], the following equations can model the mentioned cross-coupling process:

$$\varphi_f = \alpha_f + (\varphi_{f0} - \alpha_f) \exp\left(-\frac{\Delta\sigma'}{K}\right),$$

$$\frac{k}{k_0} = \left[ \frac{\alpha_f + (\varphi_{f0} - \alpha_f) \exp(-\Delta\sigma'/K)}{\varphi_{f0}} \right]^3 \quad (16)$$

where  $\Delta\sigma'$  is the change of average principal stress and  $\varphi_{f0}$  and  $k_0$  are the initial fracture porosity and permeability, respectively.

Thus, the fully coupled hydromechanical model for CO<sub>2</sub> sequestration in the coal seam is established, and the corresponding cross-couplings between the fluid transfer and coal deformation are illustrated in Figure 5. As mentioned above, during CO<sub>2</sub> injection, the increasing fluid pressure in fracture causes the opening of coal fracture and further leads to the increase of the fracture porosity, the increasing CO<sub>2</sub> pressure in the coal matrix softens the coal seam and makes the coal easier to deform, and the CO<sub>2</sub> adsorption results in obvious coal swelling, which can induce the decrease of fracture porosity. All the alternations on the mechanical field will have a substantial feedback on the hydraulic field, which is mainly reflected in coal permeability. In the next sections, the proposed model is implemented into COMSOL multiphysics software to have further validation and analysis.

### 3. Model Validation

In this section, to verify the reliability and accuracy of the new proposed model, we match the experimental data derived by Robertson and Christiansen [38] with the numerical results calculated by our model. In the experiment [38], as shown in Figure 6(a), the coal sample was confined by a constant confining pressure, and a fixed constraint was set at one end of

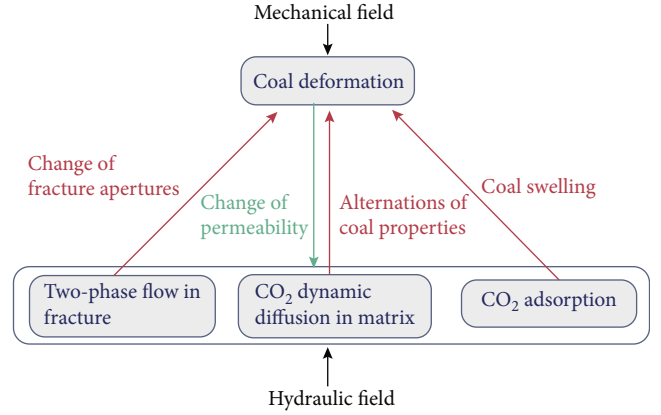


FIGURE 5: Cross-couplings between fluid transfer and coal deformation.

the sample while the CO<sub>2</sub> injection was performed at the other end of the sample. In the numerical simulation, a 2-D geometry model is developed to restore the real experimental conditions, which is illustrated in Figure 6(b).

Figure 7 depicts the comparison of coal permeability obtained by the experiment and simulation. It can be seen that the theoretical values computed by the new model are in agreement with the actual values. This result also indicates that our model is reliable and reasonable in modeling long-term CO<sub>2</sub> sequestration.

## 4. Model Application and Analyses

**4.1. Geometry Model and Definite Condition.** In order for the proposed theoretical model to account for the long-term CO<sub>2</sub> sequestration in the coal seam, a 3-D geometry model with a vertical well is assumed, which is illustrated in Figure 8(a). In the assumption, the thickness and radius of the coal seam are 15 and 1000 meters, respectively, and the injection well is located at the center of the model. Further, because of the symmetry in the established model and the complexity in computing the three-dimensional network with a finite element, we simplify the mentioned geometry model into a 2-D model, as depicted in Figure 8(b). In addition, two monitor points MA (10, 0) and MB (200, 0) are laid out to investigate the variation of multiple parameters in different conditions during the CO<sub>2</sub> injection.

In this paper, the complex coupled model is handled by a finite element method using COMSOL multiphysics software. And the essence of dealing with this problem is to solve the partial differential equations. Therefore, defining the boundary conditions of different variables is the major step in solving the provided equations. For coal deformation, the boundary conditions are shown in Figure 8(b). For CO<sub>2</sub> diffusion in the coal matrix, the boundary condition is unavailable because the corresponding governing equation does not involve the derivative of position. While for the two-phase flow in fracture, the top, bottom, and right boundaries are set with no-flow boundary, and the flux boundary condition (Neumann boundary condition) is adopted on the left side

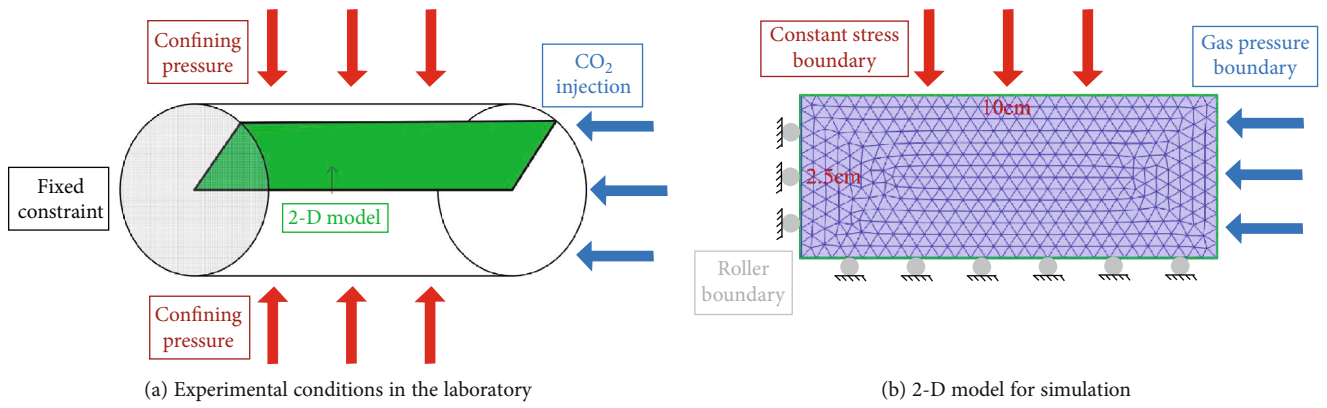


FIGURE 6: The model used in the validation.

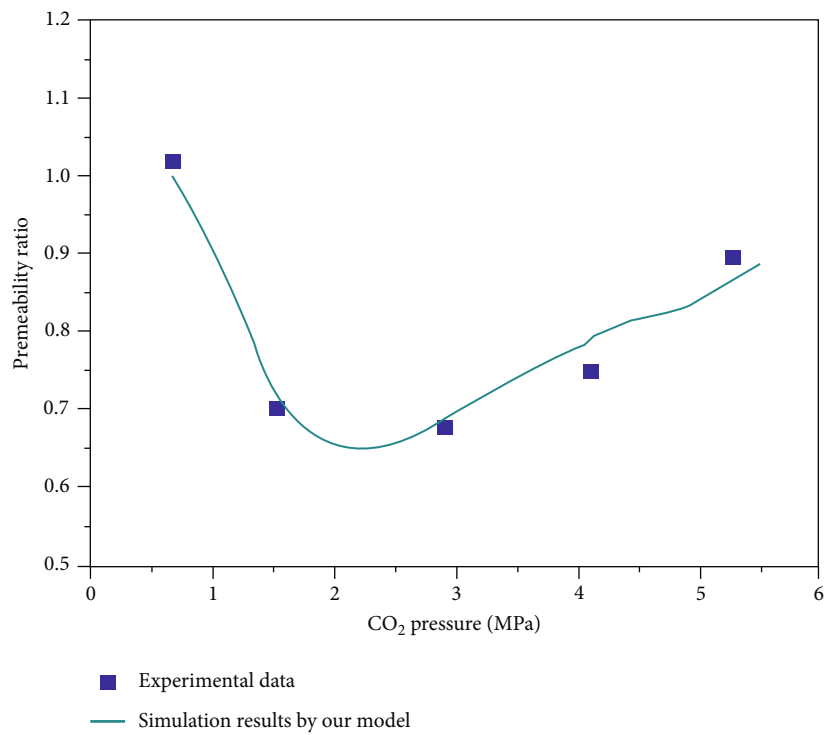


FIGURE 7: Results of coal permeability obtained by the experiment and simulation during CO<sub>2</sub> injection.

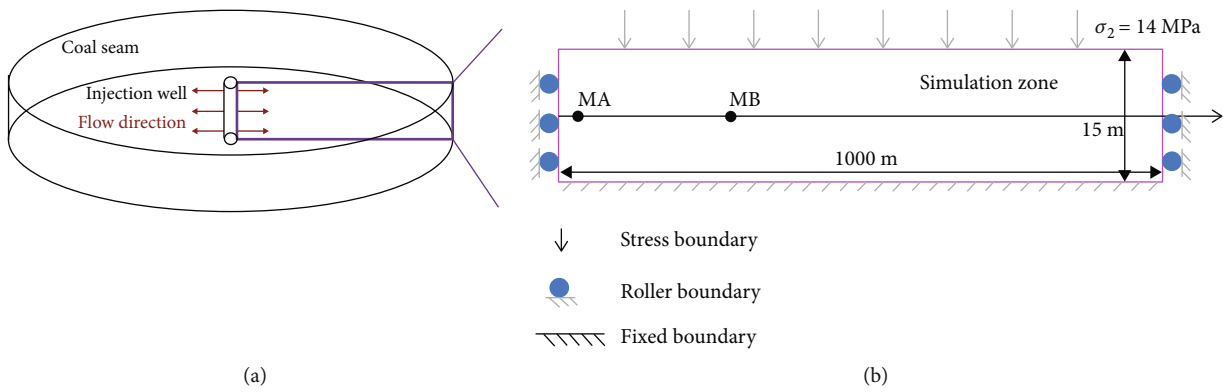


FIGURE 8: Schematic of the simulation model for long-term CO<sub>2</sub> sequestration.

of the model, which can be written as:

$$\begin{cases} \vec{n} \cdot \frac{kk_{rg}}{\mu_g} \nabla p_{fg} = Q_{fg} & \text{on } \Omega_{AB} \\ \vec{n} \cdot \frac{kk_{rw}}{\mu_w} \nabla p_{fw} = Q_{fw} & \text{on } \Omega_{AB} \end{cases} \quad (17)$$

here,  $\Omega_{AB}$  represents the boundary AB,  $\vec{n}$  represents the normal vector of the referring boundary, and  $Q_{fg}$  and  $Q_{fw}$  are the injection rate of  $\text{CO}_2$  and water per unit time, respectively. Additionally, some key parameters used in the numerical simulation are listed in Table 1.

**4.2. Simulation Results.** Figure 9 depicts the gas pressure and  $\text{CO}_2$  accumulative storage versus time during the  $\text{CO}_2$  injection. It can be found that because the  $\text{CO}_2$  injection rate is constant, the  $\text{CO}_2$  accumulative storage is directly proportional to the injection time. But at the early injection stage, the stored  $\text{CO}_2$  is mainly in an adsorbed state, while at the later injection stage, the stored  $\text{CO}_2$  is mainly in the free state due to the attenuation of  $\text{CO}_2$  diffusion in the coal matrix. Also, the decrease in diffusion coefficient blocks the gas transfer from coal fracture into the inner of the coal seam and further limits the rise of gas matrix pressure. This mechanism is more nonnegligible when it is far away from the wellhead. For instance, after a 500-day  $\text{CO}_2$  injection, the value of gas pressure in the matrix is 98.86% of that in fracture at MA, while at MB, this number decreases to 53.96%, as shown in Figure 9(b).

Coal permeability and water saturation are the two most essential parameters in controlling the two-phase flow behavior. Figures 10(a) and 10(b) present the distribution laws of the two valuables at different injection times. The results show that along the direction of injection, the value of the permeability ratio decreases firstly and then increases to the initial value. For the early stage of injection, the permeability of the affected area is below the initial value because of the adsorption-induced swelling, and for the later stage of injection, the permeability of the area adjacent to the wellbore exceeds the initial value as a result of the increasing fracture pressure. This figure also indicates that at any specific position, the permeability increases with time after a certain degree of decline. Additionally, from Figure 10(b), the water saturation increases firstly and then decreases with the increase of distance from the well. The minimum of water saturation appears at the wellhead, which is equal to the value of water residual saturation, while the maximum of water saturation occurs at the middle of the coal seam, and the distance of the corresponding position from the wellhead increases with injection time.

Young's modulus and Poisson's ratio are the two most essential parameters in controlling coal behavior during  $\text{CO}_2$  injection. Figures 10(c) and 10(d) present the distribution laws of the two valuables at different injection times. It can be found that Young's modulus decreases with injection time and increases with the distance from the injection well. However, the variation of Poisson's ratio is quite the opposite. That

TABLE 1: Parameters implemented in the simulator.

| Valuable (parameter)                                 | Value               | Units                  |
|--|---------------------|------------------------|
| $D_0$ (initial $\text{CO}_2$ diffusion coefficient)  | $5 \times 10^{-13}$ | $\text{m}^2/\text{s}$  |
| $\beta$ (attenuation coefficient)                    | $1 \times 10^{-6}$  | -                      |
| $T$ (temperature)                                    | 293                 | K                      |
| $\rho_c$ (density of coal)                           | 1650                | $\text{kg}/\text{m}^3$ |
| $v_L$ (Langmuir volume constant)                     | 0.045               | $\text{m}^3/\text{kg}$ |
| $p_L$ (Langmuir pressure constant)                   | 0.6                 | MPa                    |
| $L$ (average distance between coal fractures)        | 0.005               | m                      |
| $s_{wr}$ (water residual saturation)                 | 0.2                 | -                      |
| $s_{gr}$ (gas residual saturation)                   | 0.1                 | -                      |
| $a$ (the coefficient in Eq. (11))                    | 0.65                | -                      |
| $E$ (initial Young's modulus of coal)                | 4                   | GPa                    |
| $\nu$ (Poisson's ratio of coal with no overpressure) | 0.285               | -                      |
| $\varepsilon_L$ (Langmuir strain constant)           | 0.03                | -                      |
| $\varphi_{f0}$ (initial fracture porosity)           | 0.03                | -                      |
| $k_0$ (initial permeability)                         | $6 \times 10^{-15}$ | $\text{m}/\text{s}$    |
| $\varphi_m$ (porosity of coal matrix)                | 0.01                | -                      |
| $S_{w0}$ (initial water saturation)                  | 0.6                 | -                      |
| $Q_{fg}$ ( $\text{CO}_2$ injection rate)             | $5 \times 10^{-4}$  | $\text{m}^2/\text{s}$  |
| $Q_{fw}$ (water injection rate)                      | $5 \times 10^{-7}$  | $\text{m}^2/\text{s}$  |

means the coal seam displays a higher value of Poisson's ratio near the wellhead and at the later injection stage.

**4.3. The Impact of Multiphase Flow on the Model.** Figure 11 compares the distribution of gas pressure, coal permeability, Young's modulus, and Poisson's ratio with the two-phase flow model and single-phase flow model after 500-day injection. Because of the low compressibility of water, the model considering two-phase flow shows a higher gas pressure during the  $\text{CO}_2$  injection, which further induces the lower Young's modulus and higher Poisson's ratio for coal seam. In addition, due to the difference of Young's modulus, the coal permeability calculated by the two-phase model is higher than the single-phase model. All the mentioned rules are more notable near the injection well. This conclusion also indicates that the impact of multiphase flow on fluid transfer and coal behavior is principally reflected in the area adjacent to the wellbore.

**4.4. Impact of Gas Dynamic Diffusion on the Model.** Figure 12 compares the distribution of gas pressure, coal permeability, Young's modulus, and Poisson's ratio with the dynamic diffusion model and unipore diffusion model after 500-day injection. Because of the decrease in gas diffusion coefficient, the model considering gas dynamic diffusion shows a lower gas matrix pressure during the  $\text{CO}_2$  injection, which further induces the greater coal permeability, higher Young's modulus, and lower Poisson's ratio for coal seam. Additionally, as shown in Figure 12(a), the impact of the gas dynamic diffusion on gas matrix pressure and fracture pressure is quite the opposite. This is because for the multistage pore model, fewer  $\text{CO}_2$  molecules are allowed to diffuse into the coal matrix, and more  $\text{CO}_2$  molecules are stranded in the coal

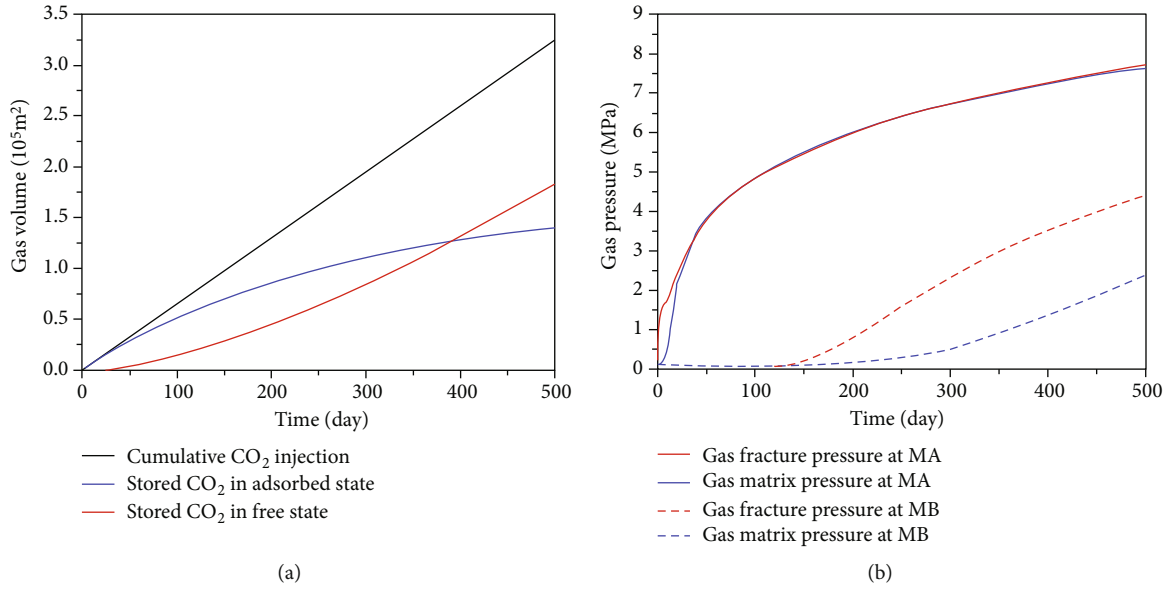


FIGURE 9: The variation of (a) cumulative CO<sub>2</sub> injection and (b) gas pressure of matrix and fracture at MA and MB during 500 days of injection.

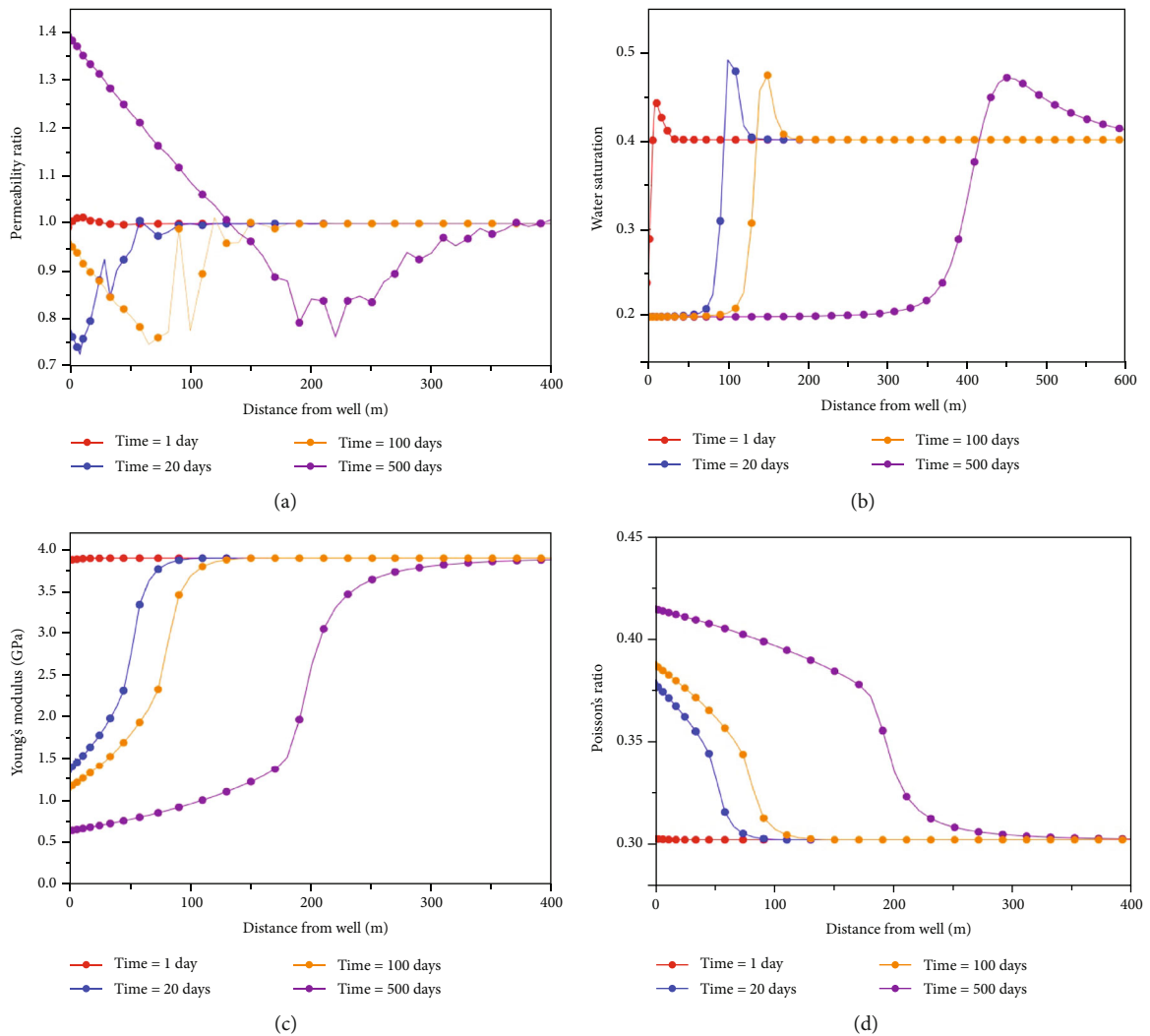


FIGURE 10: The spatial distribution of (a) permeability ratio, (b) water saturation, (c) Young's modulus, and (d) Poisson's ratio after 1 day, 20 days, 100 days, and 500 days of injection.

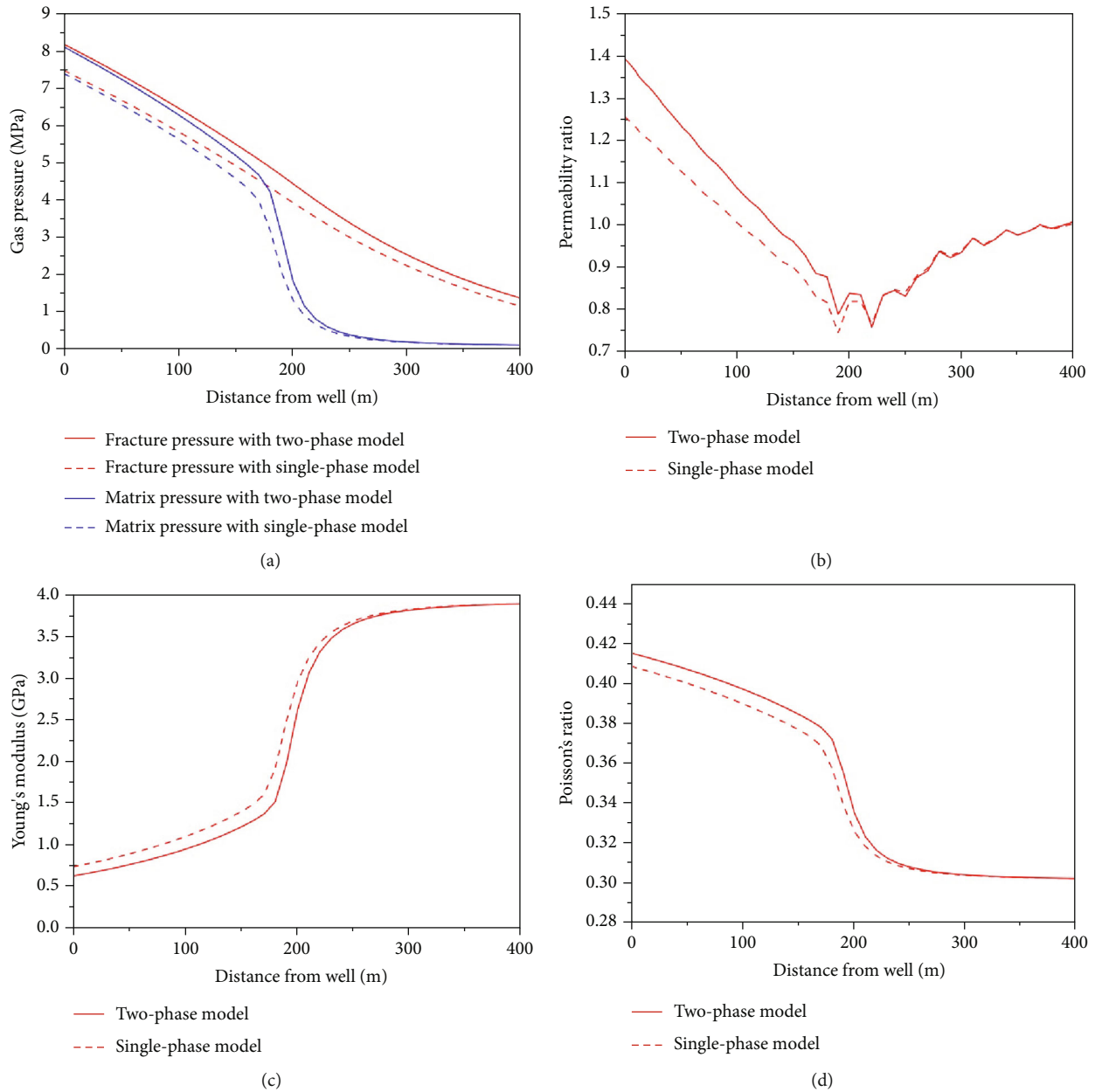


FIGURE 11: Impact of multiphase flow on fluid transfer and coal behavior.

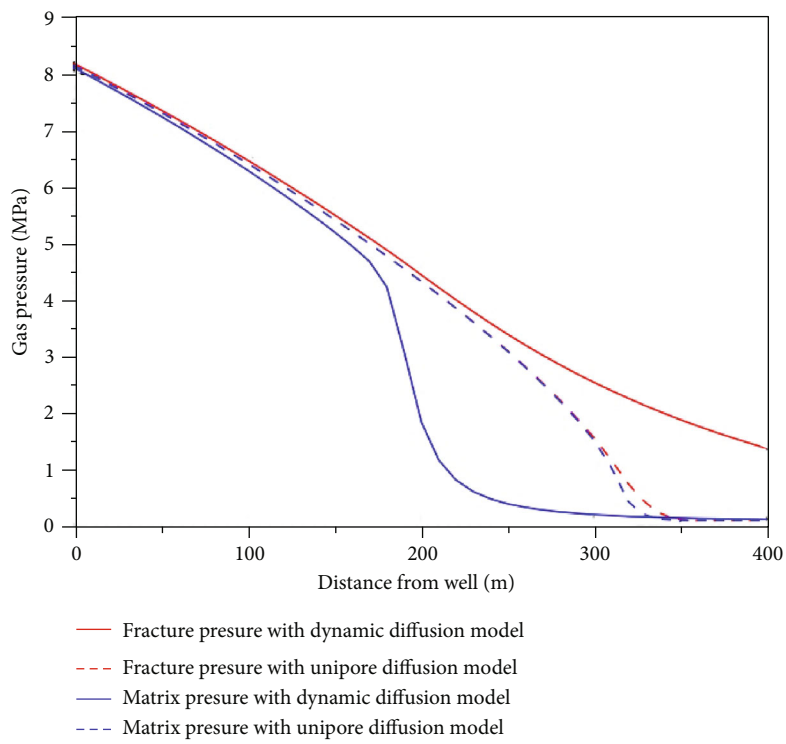
fracture. The figure also indicates that the impact of the gas dynamic diffusion on fluid transfer and coal behavior is principally reflected in the area far away from the wellhead.

## 5. Conclusions

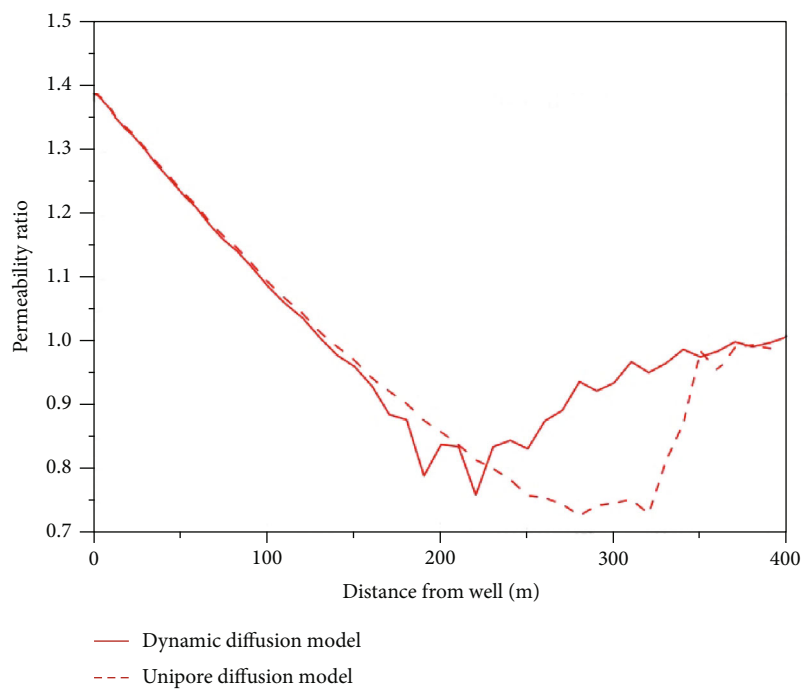
In this paper, we numerically studied the fluid transfer and coal behavior during  $\text{CO}_2$  sequestration in an unminable coal seam. To comprehensively describe the whole process, a multistage  $\text{CO}_2$  diffusion model is adopted and a fully coupled hydromechanical model is developed. In the proposed models, the two-phase flow in fracture, the multistage pore structure of the coal matrix, the adsorption-induced coal swelling, and the  $\text{CO}_2$ -induced coal softening are also considered, which is controlled by four governing equations and

several cross-coupling equations. These equations are solved by COMSOL multiphysics software with the finite element method. In addition, through the model validation, application, and analysis, the following conclusions can be drawn:

- (1) Our new proposed model is well varied by the experimental data. It is more applicable and accurate in modeling long-term  $\text{CO}_2$  sequestration in coal seam
- (2) At the early injection stage, the stored  $\text{CO}_2$  in the coal seam is mainly in an adsorbed state, while at the later injection stage, the stored  $\text{CO}_2$  is mainly in a free state. After 500 days of injection, the value of gas pressure in the matrix is only about 54% of that in fracture, which is attributed to the decrease in the

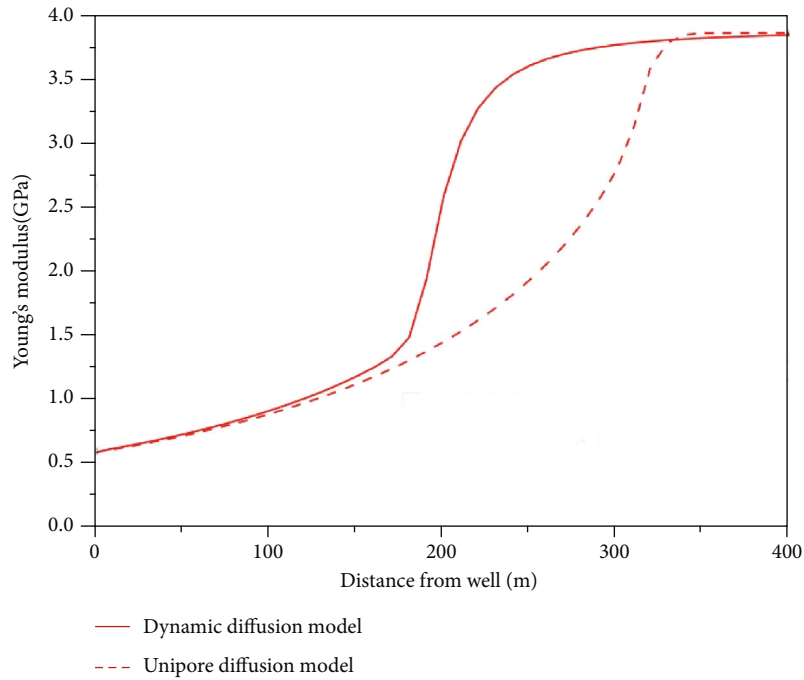


(a)

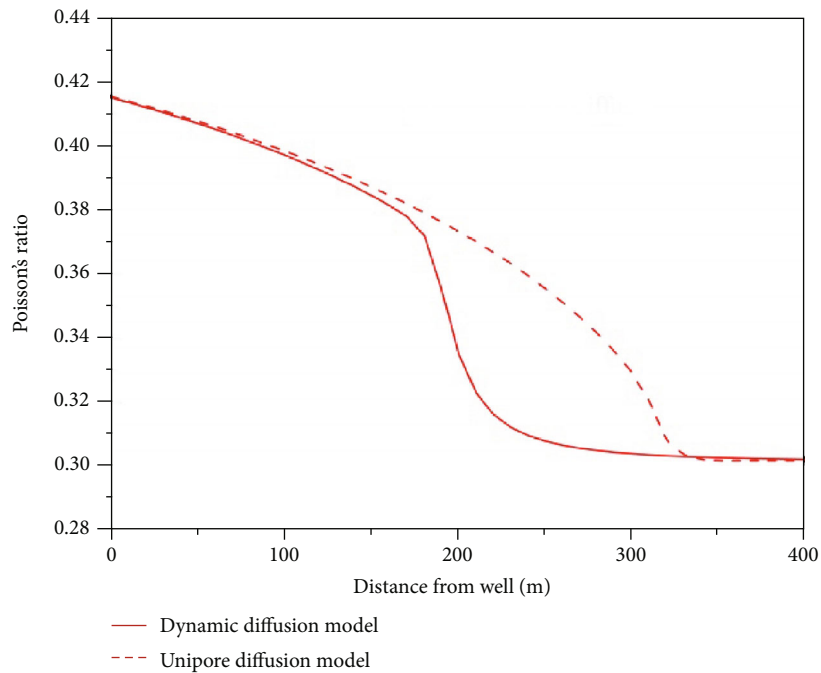


(b)

FIGURE 12: Continued.



(c)



(d)

FIGURE 12: Impact of dynamic diffusion on fluid transfer and coal behavior.

diffusion coefficient. Additionally, during CO<sub>2</sub> injection, the increasing distance from the injection well corresponds to greater water saturation, higher Young's modulus, and lower Poisson's ratio, while the coal permeability decreases firstly and then increases with the distance from the wellhead

(3) The impact of multiphase flow on fluid transfer and coal behavior is principally embodied in the area

adjacent to the injection well. Further, the model considering the multiphase flow shows a greater permeability, a lower Young's modulus, and a higher Poisson's ratio for coal seam. That also means the coal seam with lower water content is more reliable for long-term CO<sub>2</sub> sequestration

(4) The impact of the gas dynamic diffusion on fluid transfer and coal behavior is principally embodied

in the area far away from the injection well. Further, the model considering gas dynamic diffusion shows a greater permeability, a higher Young's modulus, and a lower Poisson's ratio for coal seam. That also means the coal seam with greater attenuation coefficient of CO<sub>2</sub> diffusion is more reliable for long-term CO<sub>2</sub> sequestration

Additionally, the temperature of injection CO<sub>2</sub> also has a significant impact on fluid flow and coal behavior, which needs to be investigated in the future.

## Data Availability

Data are available on request.

## Conflicts of Interest

The authors declare that they have no conflicts of interest.

## Acknowledgments

This study was supported by the Postgraduate Research & Practice Innovation Program of Jiangsu Province (No. KYCX20\_1980) and the Future Scientists Program of China University of Mining and Technology (No. 2020WLKXJ055).

## References

- [1] J. D. Figueroa, T. Fout, S. Plasynski, H. McIlvried, and R. D. Srivastava, "Advances in CO<sub>2</sub> capture technology—the U.S. Department of Energy's carbon sequestration program," *International Journal of Greenhouse Gas Control*, vol. 2, no. 1, pp. 9–20, 2008.
- [2] R. S. Haszeldine, "Carbon capture and storage: how green can black be?," *Science*, vol. 325, no. 5948, pp. 1647–1652, 2009.
- [3] T. Ma, J. Rutqvist, C. M. Oldenburg, and W. Liu, "Coupled thermal-hydrological-mechanical modeling of CO<sub>2</sub>-enhanced coalbed methane recovery," *International Journal of Coal Geology*, vol. 179, pp. 81–91, 2017.
- [4] F. Qanbari, M. Pooladi-Darvish, S. H. Tabatabaie, and S. Gerami, "CO<sub>2</sub> disposal as hydrate in ocean sediments," *Journal of Natural Gas Science and Engineering*, vol. 8, pp. 139–149, 2012.
- [5] E. Nduagu, J. Bergerson, and R. Zevenhoven, "Life cycle assessment of CO<sub>2</sub> sequestration in magnesium silicate rock - a comparative study," *Energy Conversion and Management*, vol. 55, pp. 116–126, 2012.
- [6] C. M. White, D. H. Smith, K. L. Jones et al., "Sequestration of carbon dioxide in coal with enhanced coalbed methane recovery a review†," *Energy & Fuels*, vol. 19, no. 3, pp. 659–724, 2005.
- [7] M. S. Masoudian, A. El-Zein, and D. W. Airey, "Modelling stress and strain in coal seams during CO<sub>2</sub> injection incorporating the rock-fluid interactions," *Computers and Geotechnics*, vol. 76, pp. 51–60, 2016.
- [8] R. Shukla, P. Ranjith, A. Haque, and X. Choi, "A review of studies on CO<sub>2</sub> sequestration and caprock integrity," *Fuel*, vol. 89, no. 10, pp. 2651–2664, 2010.
- [9] K. H. S. M. Sampath, M. S. A. Perera, P. G. Ranjith, and S. K. Matthai, "CO<sub>2</sub> interaction induced mechanical characteristics alterations in coal: a review," *International Journal of Coal Geology*, vol. 204, pp. 113–129, 2019.
- [10] Y. Wu, J. Liu, D. Elsworth, Z. Chen, L. Connell, and Z. Pan, "Dual poroelastic response of a coal seam to CO<sub>2</sub> injection," *International Journal of Greenhouse Gas Control*, vol. 4, no. 4, pp. 668–678, 2010.
- [11] H. Qu, J. Liu, Z. Chen et al., "Complex evolution of coal permeability during CO<sub>2</sub> injection under variable temperatures," *International Journal of Greenhouse Gas Control*, vol. 9, pp. 281–293, 2012.
- [12] M. S. Masoudian, D. W. Airey, and A. El-Zein, "The role of coal seam properties on coupled processes during CO<sub>2</sub> sequestration: a parametric study," *Greenhouse Gases: Science and Technology*, vol. 6, no. 4, pp. 492–518, 2016.
- [13] Y. P. Fan, C. B. Deng, X. Zhang, F. Q. Li, X. Y. Wang, and L. Qiao, "Numerical study of CO<sub>2</sub>-enhanced coalbed methane recovery," *International Journal of Greenhouse Gas Control*, vol. 76, pp. 12–23, 2018.
- [14] R. Zhang, X. Yin, P. H. Winterfeld, and Y.-S. Wu, "A fully coupled thermal-hydrological-mechanical-chemical model for CO<sub>2</sub> geological sequestration," *Journal of Natural Gas Science and Engineering*, vol. 28, pp. 280–304, 2016.
- [15] C. Fan, D. Elsworth, S. Li, L. Zhou, Z. Yang, and Y. Song, "Thermo-hydro-mechanical-chemical couplings controlling CH<sub>4</sub> production and CO<sub>2</sub> sequestration in enhanced coalbed methane recovery," *Energy*, vol. 173, pp. 1054–1077, 2019.
- [16] D. Huo and S. M. Benson, "Experimental investigation of stress-dependency of relative permeability in rock fractures," *Transport in Porous Media*, vol. 113, no. 3, pp. 567–590, 2016.
- [17] N. Watanabe, T. Kikuchi, and T. Ishibashi, "v-X-type relative permeability curves for steam-water two-phase flows in fractured geothermal reservoirs," *Geothermics*, vol. 65, pp. 269–279, 2017.
- [18] M. Fahad, F. Hussain, S. S. Rahman, and Y. Cinar, "Experimental investigation of upscaling relative permeability for two phase flow in fractured porous media," *Journal of Petroleum Science and Engineering*, vol. 149, pp. 367–382, 2017.
- [19] D. B. Bennion and S. Bachu, "Permeability and relative permeability measurements at reservoir conditions for CO<sub>2</sub>-water systems in ultra low permeability confining caprocks," in *In Proceedings of EUROPEC/EAGE Conference and Exhibition*, p. 9, London, U.K, January 2007.
- [20] P. Q. Lian, L. S. Cheng, and C. Y. Ma, "The characteristics of relative permeability curves in naturally fractured carbonate reservoirs," *Journal of Canadian Petroleum Technology*, vol. 51, no. 2, pp. 137–142, 2013.
- [21] X. Pan, R. C. Wong, and B. B. Maini, "Steady state two-phase in a smooth parallel fracture," in *Proceedings of Annual Technical Meeting*, p. 12, Calgary, Alberta, January 1996.
- [22] A. T. Corey, "The interrelation between gas and oil relative permeability," *Producers Monthly*, vol. 19, pp. 38–41, 1954.
- [23] R. H. Brooks and A. T. Corey, "Properties of porous media affecting fluid flow," *Journal of the Irrigation and Drainage Division*, vol. 92, pp. 61–90, 1966.
- [24] J. Kang, F. Zhou, T. Xia, and G. Ye, "Numerical modeling and experimental validation of anomalous time and space subdiffusion for gas transport in porous coal matrix," *International Journal of Heat and Mass Transfer*, vol. 100, pp. 747–757, 2016.
- [25] T. Liu, B. Lin, X. Fu et al., "Experimental study on gas diffusion dynamics in fractured coal: a better understanding of gas

- migration in in-situ coal seam,” *Energy*, vol. 195, p. 117005, 2020.
- [26] R. Yang, T. Ma, H. Xu, W. Liu, Y. Hu, and S. Sang, “A model of fully coupled two-phase flow and coal deformation under dynamic diffusion for coalbed methane extraction,” *Journal of Natural Gas Science and Engineering*, vol. 72, p. 103010, 2019.
- [27] T. Liu, B. Lin, W. Yang et al., “Dynamic diffusion-based multi-field coupling model for gas drainage,” *Journal of Natural Gas Science and Engineering*, vol. 44, pp. 233–249, 2017.
- [28] C. R. Clarkson and R. M. Bustin, “The effect of pore structure and gas pressure upon the transport properties of coal: a laboratory and modeling study. 2. Adsorption rate modeling,” *Fuel*, vol. 78, no. 11, pp. 1345–1362, 1999.
- [29] Z. Liu, Y. Cheng, L. Wang, B. Pang, W. Li, and J. Jiang, “Experimental investigation of the constant and time-dependent dynamic diffusion coefficient: implication for CO<sub>2</sub> injection method,” *Fuel*, vol. 267, p. 117283, 2020.
- [30] J. Zhao, D. Tang, Y. Qin, and H. Xu, “Fractal characterization of pore structure for coal macrolithotypes in the Hancheng area, southeastern Ordos Basin, China,” *Journal of Petroleum Science and Engineering*, vol. 178, pp. 666–677, 2019.
- [31] Z. Liu, H. Yang, W. Y. Wang, W. M. Cheng, and L. Xin, “Experimental study on the pore structure fractals and seepage characteristics of a coal sample around a borehole in coal seam water infusion,” *Transport in Porous Media*, vol. 125, no. 2, pp. 289–309, 2018.
- [32] Z. Q. Li, Y. Liu, Y. P. Xu, and D. Y. Song, “Gas diffusion mechanism in multi-scale pores of coal particles and new diffusion model of dynamic diffusion coefficient,” *Journal of China Coal Society*, vol. 41, pp. 633–643, 2016.
- [33] T. Liu and B. Lin, “Time-dependent dynamic diffusion processes in coal: model development and analysis,” *International Journal of Heat and Mass Transfer*, vol. 134, pp. 1–9, 2019.
- [34] Q. Q. Liu, Y. P. Cheng, H. X. Zhou, P. K. Guo, F. H. An, and H. D. Chen, “A mathematical model of coupled gas flow and coal deformation with gas diffusion and Klinkenberg effects,” *Rock Mechanics and Rock Engineering*, vol. 48, no. 3, pp. 1163–1180, 2015.
- [35] W. C. Zhu, C. H. Wei, J. Liu, H. Y. Qu, and D. Elsworth, “A model of coal-gas interaction under variable temperatures,” *International Journal of Coal Geology*, vol. 86, no. 2-3, pp. 213–221, 2011.
- [36] T. Ma, J. Rutqvist, C. M. Oldenburg, W. Liu, and J. Chen, “Fully coupled two-phase flow and poromechanics modeling of coalbed methane recovery: impact of geomechanics on production rate,” *Journal of Natural Gas Science and Engineering*, vol. 45, pp. 474–486, 2017.
- [37] T. Ma, J. Rutqvist, W. Liu, L. Zhu, and K. Kim, “Modeling of CO<sub>2</sub> sequestration in coal seams: role of CO<sub>2</sub>-induced coal softening on injectivity, storage efficiency and caprock deformation,” *Greenhouse Gases: Science and Technology*, vol. 7, no. 3, pp. 562–578, 2017.
- [38] E. P. Robertson and R. L. Christiansen, “Modeling laboratory permeability in coal using Sorption-Induced Strain Data,” *SPE Reservoir Evaluation & Engineering*, vol. 10, no. 3, pp. 260–269, 2007.